UV Stimulated Manganese Dioxide for the Persulfate Catalytic Degradation of Bisphenol A

(Supplementary Materials)

Guihua Dong[1], Bing Chen[1]*, Bo Liu[1], Stanislav R. Stoyanov[2]*, Yiqi Cao[1], Min Yang[1], Baiyu Zhang[1]

[1]Northern Region Persistent Organic Pollution Control (NRPOP) Laboratory, Faculty of Engineering and Applied Science, Memorial University of Newfoundland, St. John's, NL A1B 3X5, Canada

[2]Natural Resources Canada, CanmetENERGY Devon, 1 Oil Patch Drive, Devon, AB T9G 1A8, Canada

*Corresponding authors: Bing Chen (bchen@mun.ca) and Stanislav R. Stoyanov (stanislav.stoyanov@canada.ca)

Summary

Text S1. Persulfate detection methods

The persulfate concentration was determined by a modified spectrophotometric method. 0.5 M potassium iodide with bicarbonate buffer ($NaHCO_3$, 0.05 M) was prepared, and then 0.3 mL filtered sample was mixed with the above iodide solution (4.7 mL). Shaking well, and after 20 min reaction, the water sample was detected by spectrophotometer (UV-Vis) at λ = 352 nm.

Text S2. Characterization of MnO_2 particles

An X-ray powder diffractometer (XRD, Rigaku XtaLAB Synergy-S) was applied to determine the crystallographic structure of MnO_2 particles before and after treatment in MnO_2/UV/PS process. The surface morphology of MnO_2 particles before and after treatment in MnO_2/UV/PS process was measured by the scanning electron microscope (SEM, Quanta 400 MLA) equipped with energy-dispersive X-ray spectroscopy (EDS).

Text S3. BPA derivatization and GC-MS analysis methods

We prepared six identical mixtures, each containing: 200 mL of water containing 30 mg/L BPA, 1 mM of PS, and 0.25 g/L MnO_2. Samples (30 mL) of each were taken from different flasks after 0, 5, 15, 30, 60, 90, and 120 min of UV treatment. Each sample was transferred into a separatory funnel, and 15 mL methylene chloride was immediately added to extract the BPA and its degradation intermediates. After agitation, the mixture was allowed to settle for 30 min, and the underlying organic phase was separated from the aqueous phase. A second 15 mL aliquot of methylene chloride was then used to recover any organic matter remaining in the separatory

funnel. The extract was dehydrated with anhydrous sodium sulfate, filtered, and concentrated to near dryness on a vacuum rotary evaporator. The residue was redissolved in 1 mL of toluene and transferred to a 1.5 mL brown vial, from which a 100 μL aliquot was analyzed directly, and the remaining sample was derivatized before analysis. For derivatization, toluene was first removed from the remaining sample by evaporation to dryness under a gentle nitrogen stream, then 150 μL of BSTFA+TMCS were added to silylate the polar degradation products in the residue. The silylation reaction was conducted by heating the mixture in a water bath for 2 h at 60 ℃. Toluene (350 μL) was added to the vial to dissolve the silylated products. Both the silylated and non-silylated aliquots were analyzed using gas chromatography. Chromatographic separation of analytes was carried out using a DB-5MS UI fused silica capillary column (30 m × 0.25 mm × 0.25 μm). The inlet and detector temperatures of the gas chromatograph were set to 260 and 320 °C, respectively. The oven temperature was initially set to 80 °C and held for 3 min, then increased to 300 °C at 3 °C/min and held for 30 min. Helium was used as the carrier gas at the flow rate of 1.0 mL/min. The sample (2 μL) was injected in the pulsed splitless mode. The temperatures of the transfer line, ion source, and mass spectrometry detector were 280, 230, and 150 °C, respectively. Qualitative analysis was performed in the electron impact mode at 70 eV using the full scan mode in the m/z range of 40–1000 [1, 2].

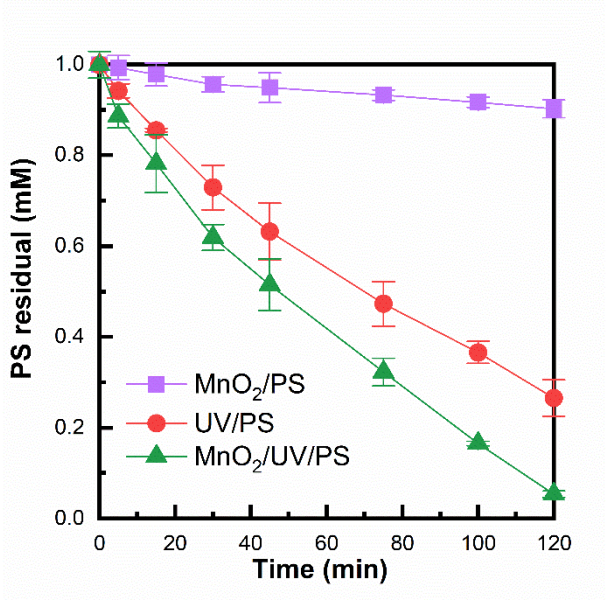

Figure S1. PS residual in MnO_2/PS, UV/PS, and MnO_2/UV/PS processes

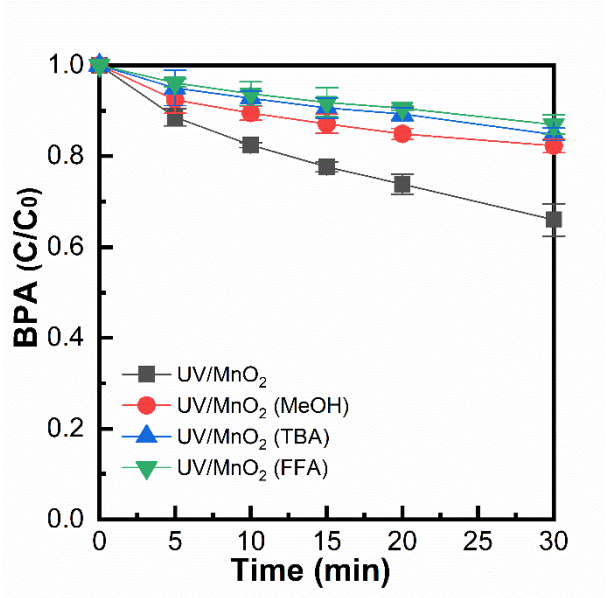

Figure S2. Effects of radical inhibitors on BPA concentrations over 30 min for UV/MnO_2. Initial conditions: [BPA] = 30 mg/L, Ph = 6.5, [PS] = 1 mM, [MnO_2] = 0.25 g/L. When inhibitor is used, initial [MeOH] = 1 M or [TBA] = 1 M or [FFA] = 5 mM.

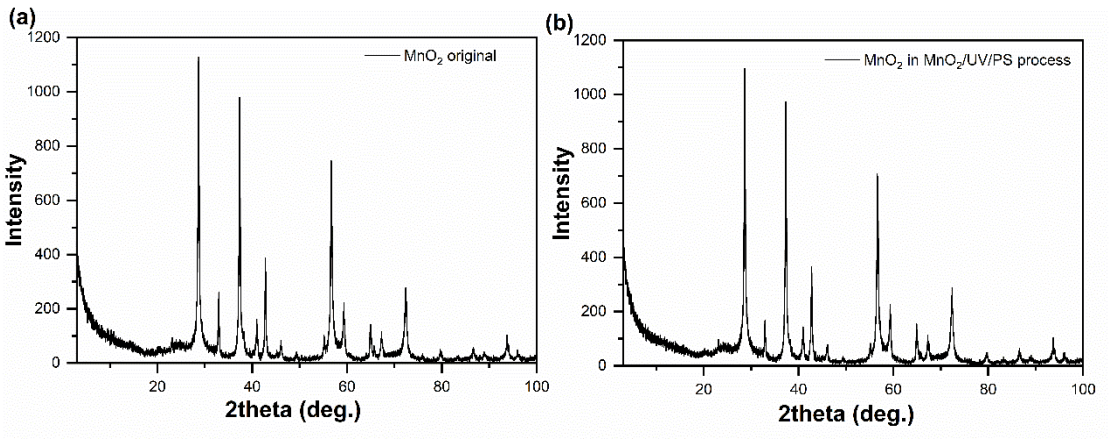

Figure S3. XRD of MnO_2 before (a) and after (b) 2 h treatment in MnO_2/UV/PS process

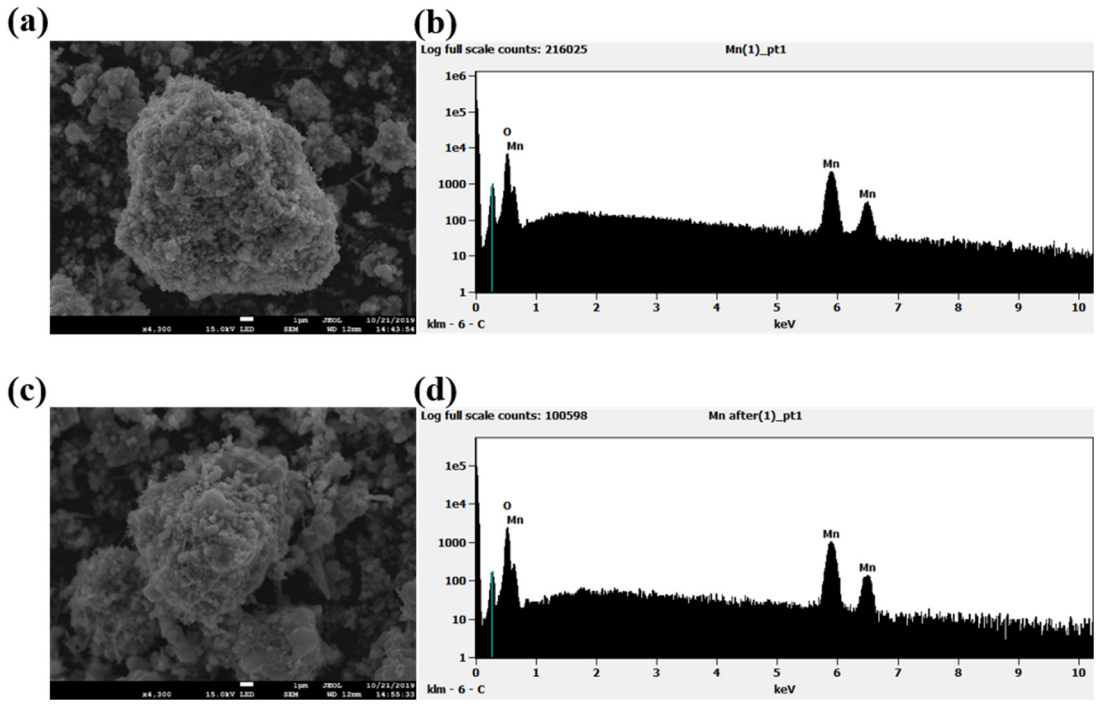

Figure S4. SEM image and EDS analysis of MnO_2 before (a, b) and after (c, d) 2 h treatment in MnO_2/UV/PS process

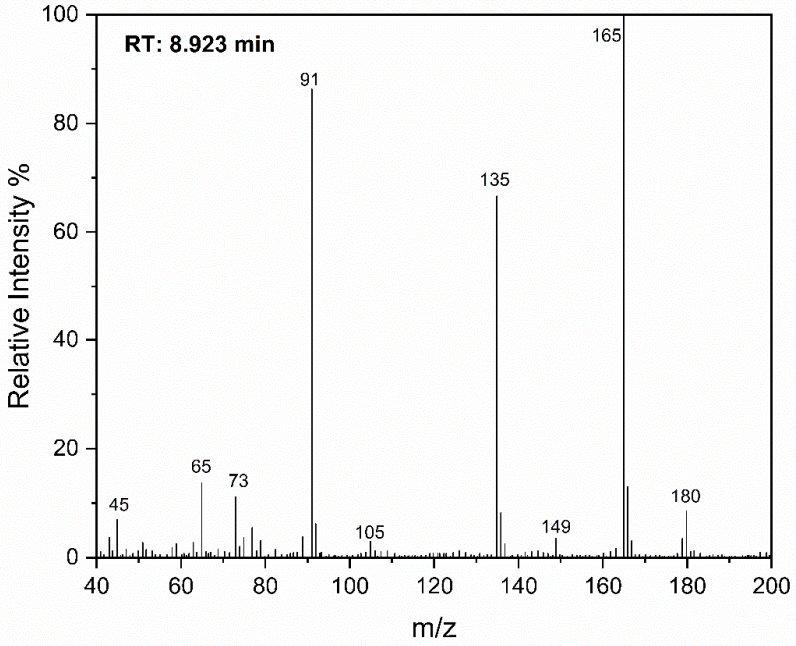
RT: 8.923 min
Relative Intensity %
m/z
100
80
60
40
20
0
40
60
80
100
120
140
160
180
200
165
91
135
65
73
45
105
149
180

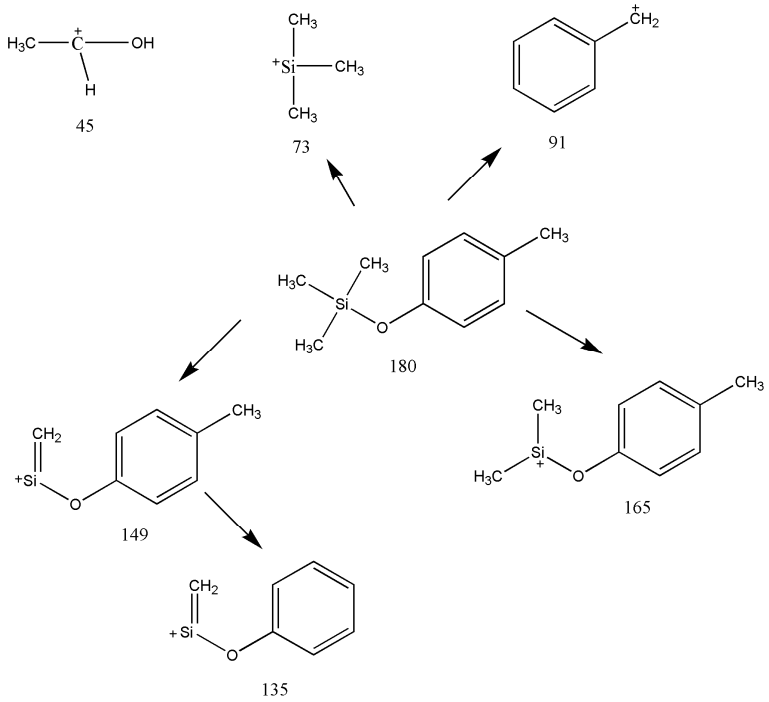
45
73
91
180
149
165
135

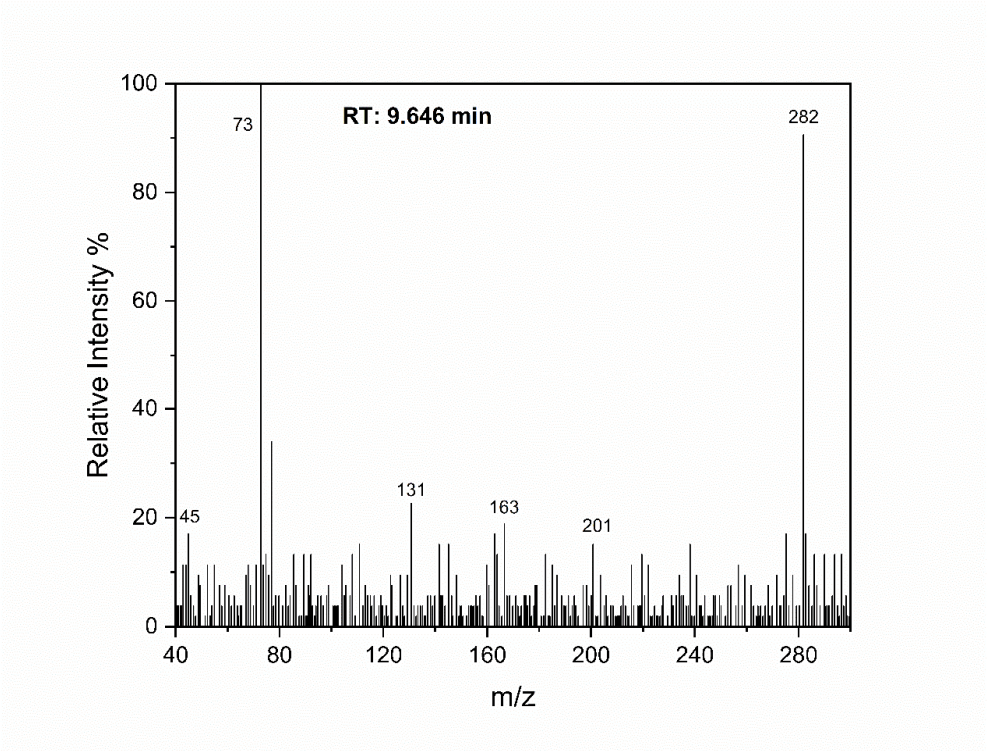
RT: 9.646 min
Relative Intensity %
m/z
73
282
131
163
201
45
100
80
60
40
20
0
40
80
120
160
200
240
280

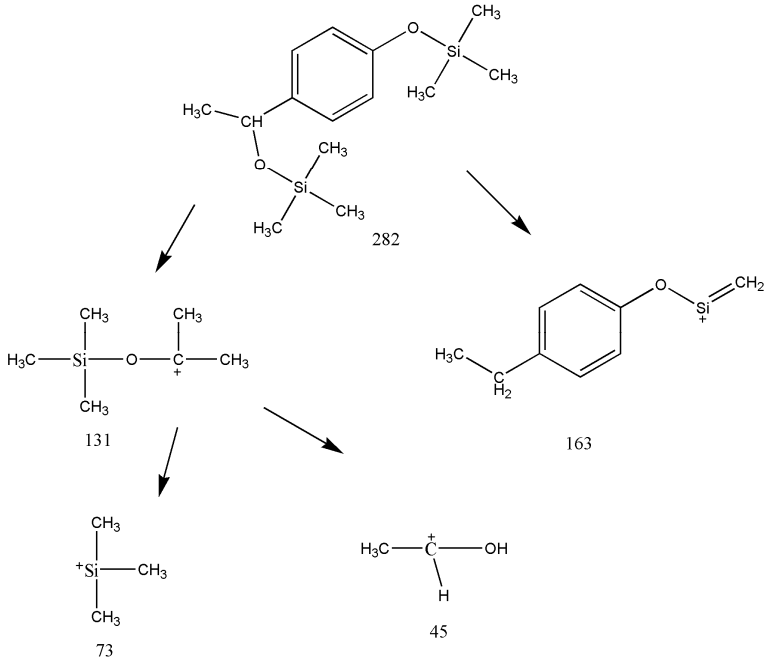
282
131
163
73
45

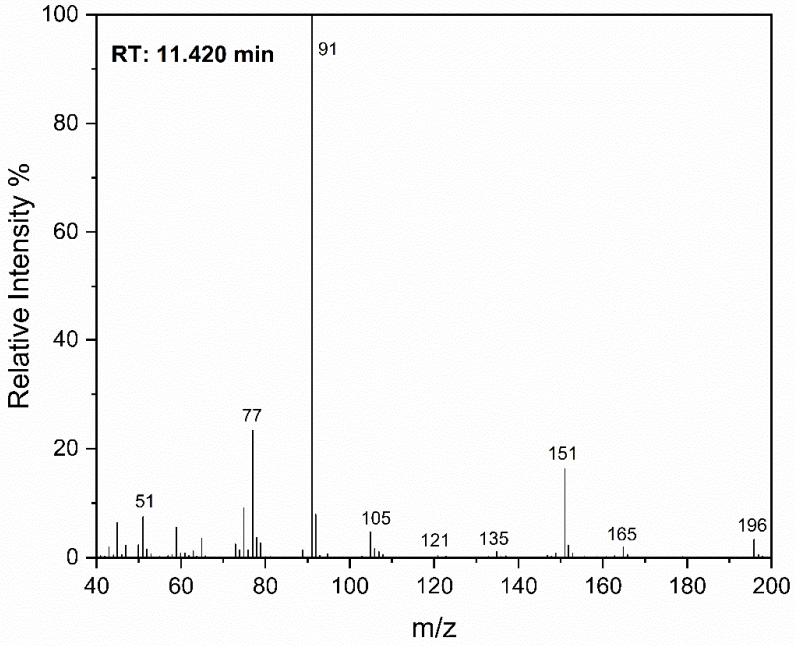
RT: 11.420 min
Relative Intensity %
m/z
91
77
51
105
121
135
151
165
196

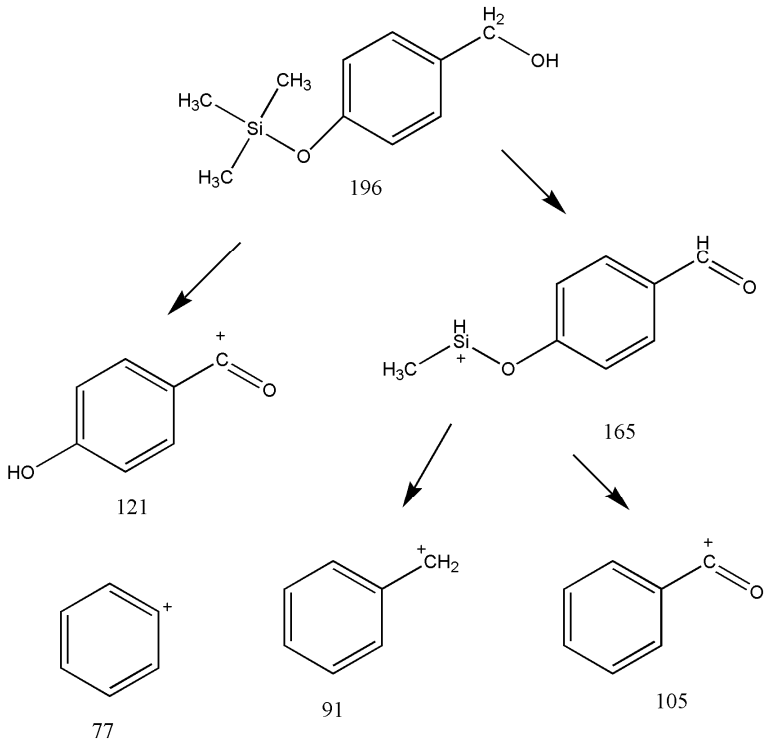
196
121
165
77
91
105

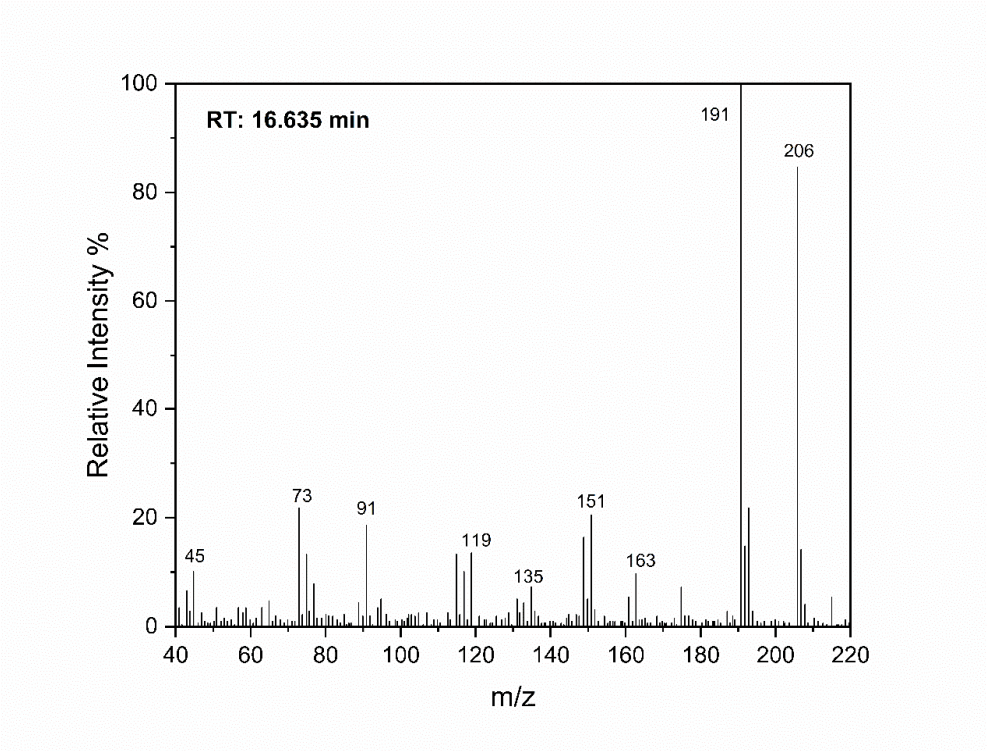
RT: 16.635 min
Relative Intensity %
m/z
100
80
60
40
20
0
40
60
80
100
120
140
160
180
200
220
191
206
73
91
151
119
163
135
45

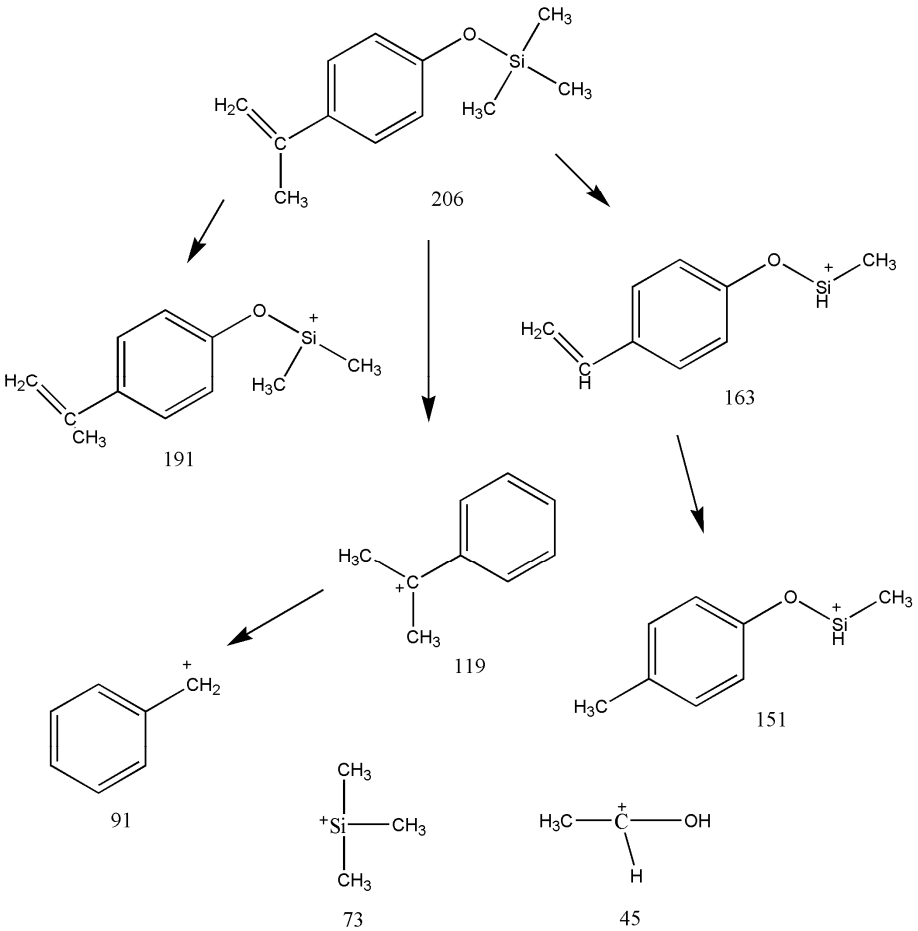
206
191
163
119
151
91
73
45

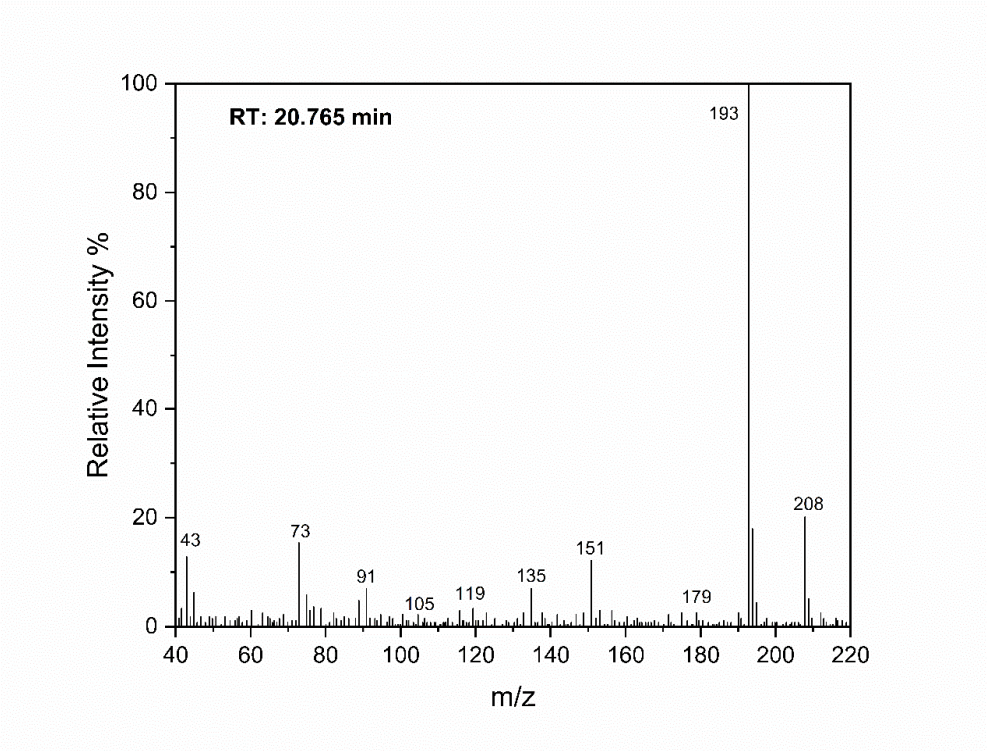
RT: 20.765 min
Relative Intensity %
m/z
193
208
73
43
151
91
135
119
105
179

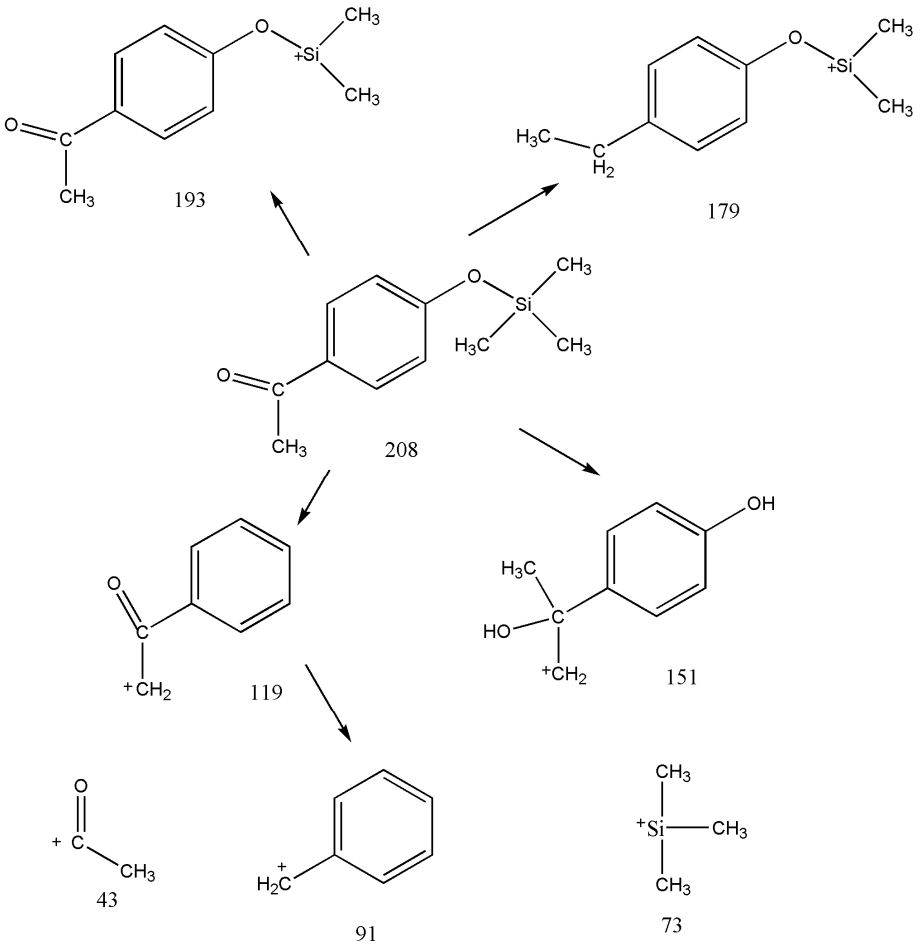
193
179
208
119
151
43
91
73

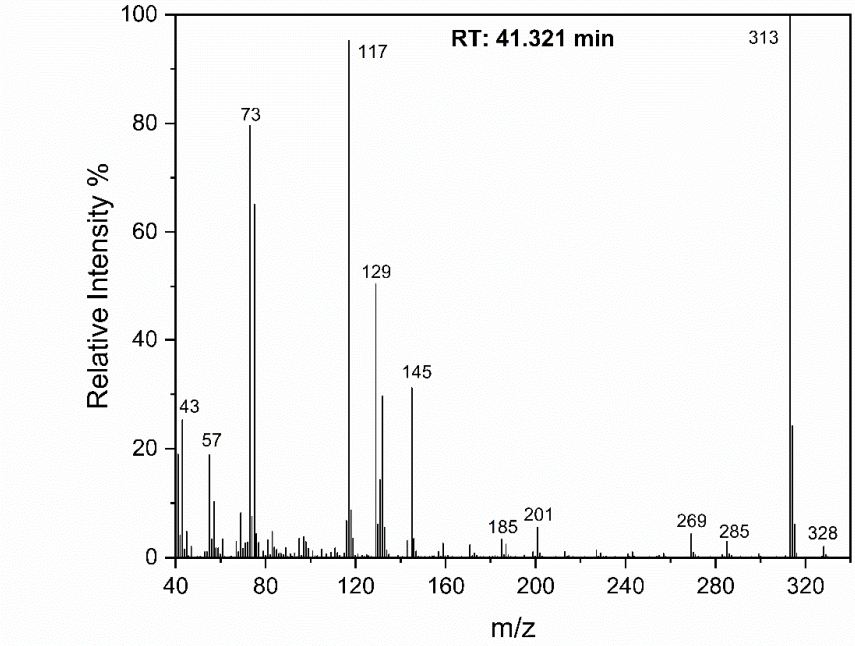

328

313

201

145

117

73

43

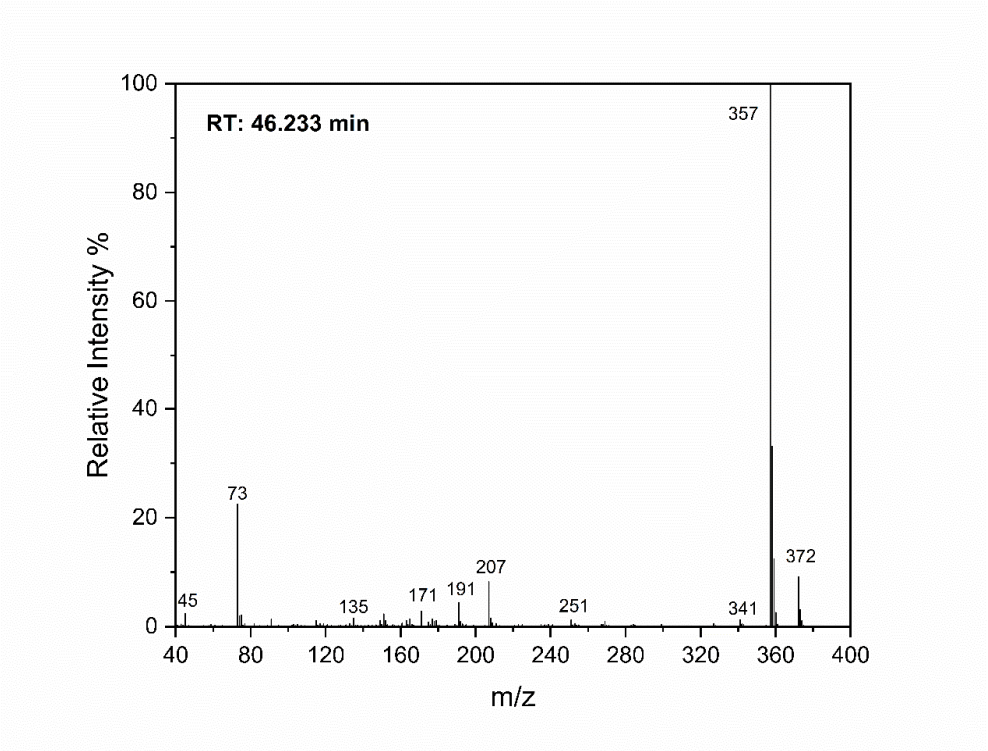
RT: 46.233 min
Relative Intensity %
m/z
357
73
372
207
191
171
135
45
251
341

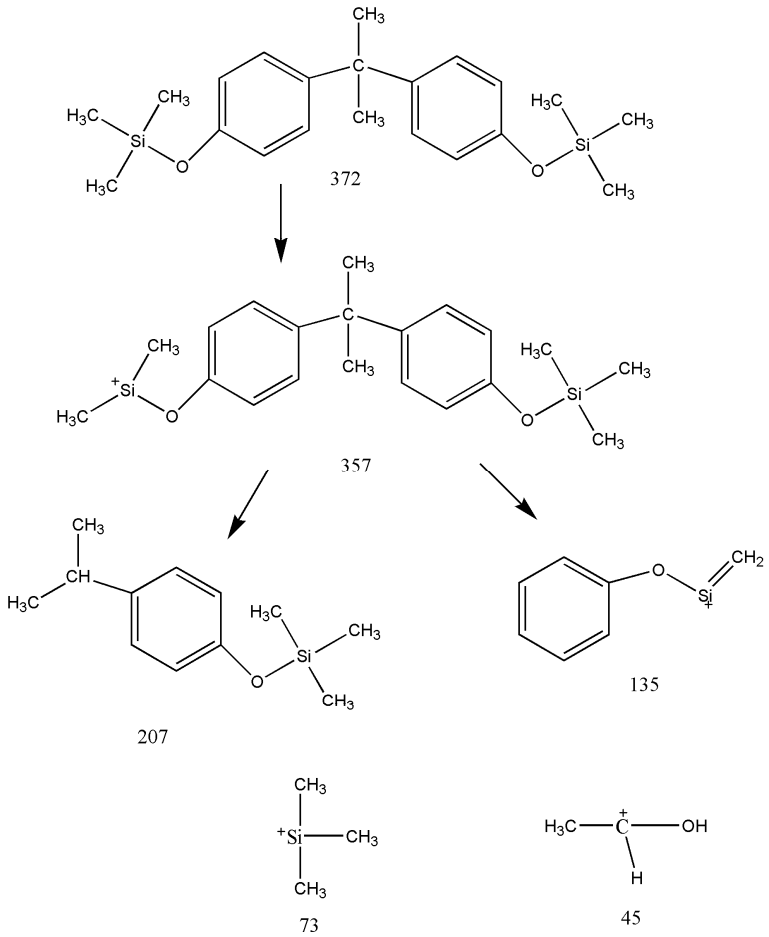
372
357
207
135
73
45

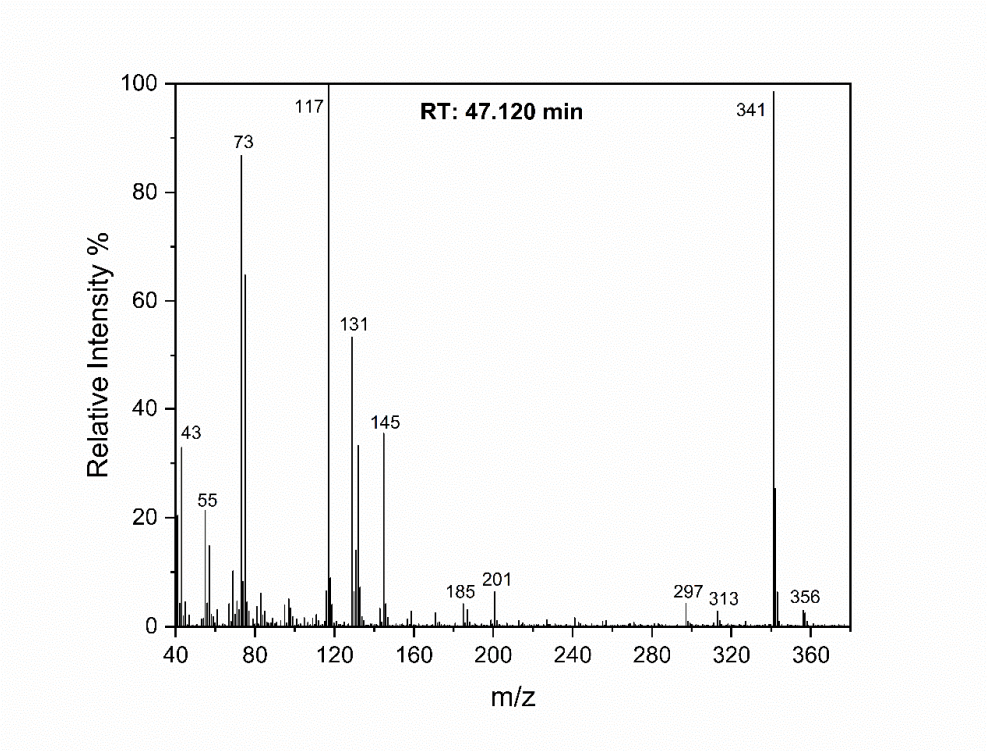
RT: 47.120 min
Relative Intensity %
m/z
100
80
60
40
20
0
40
80
120
160
200
240
280
320
360
117
73
131
145
43
55
185
201
297
313
341
356

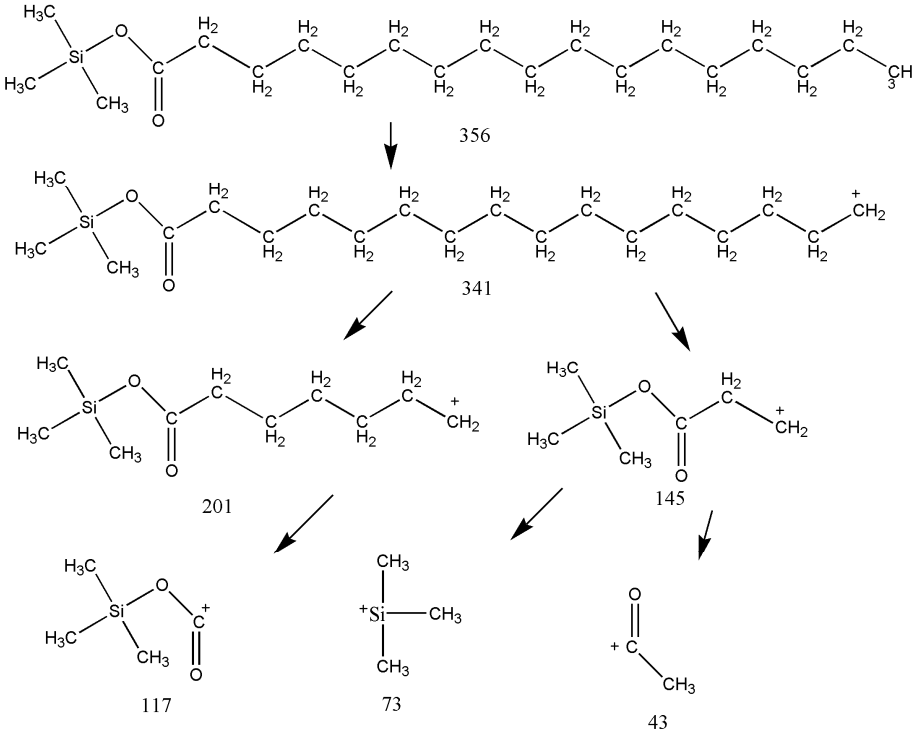
356
341
201
145
117
73
43

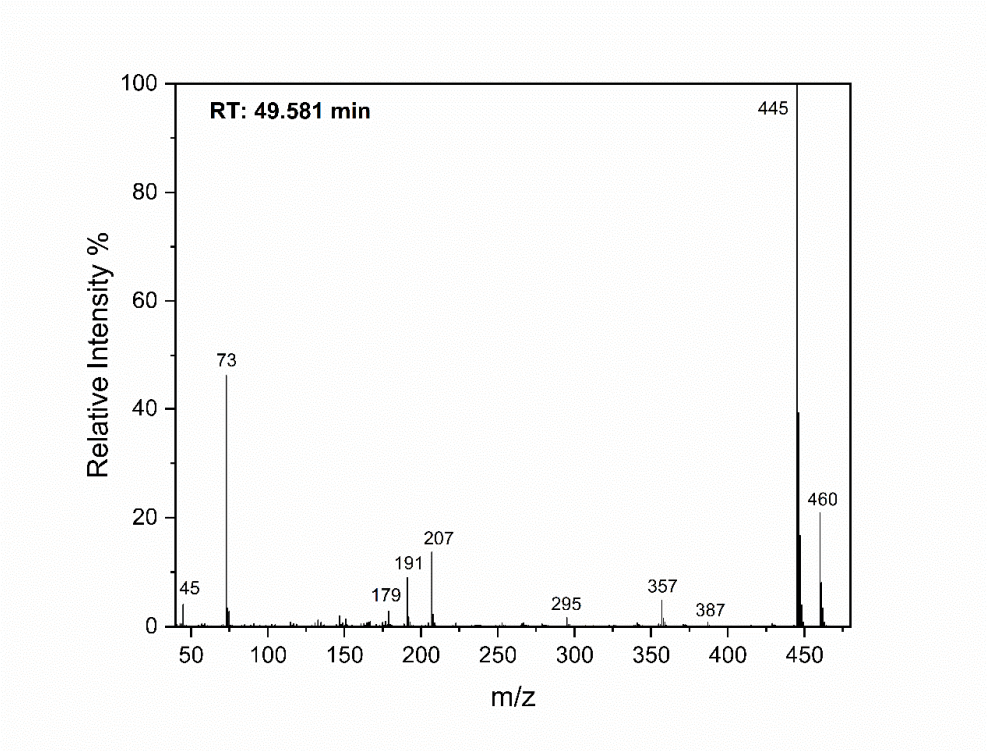
RT: 49.581 min
Relative Intensity %
m/z
445
460
73
207
191
179
45
295
357
387

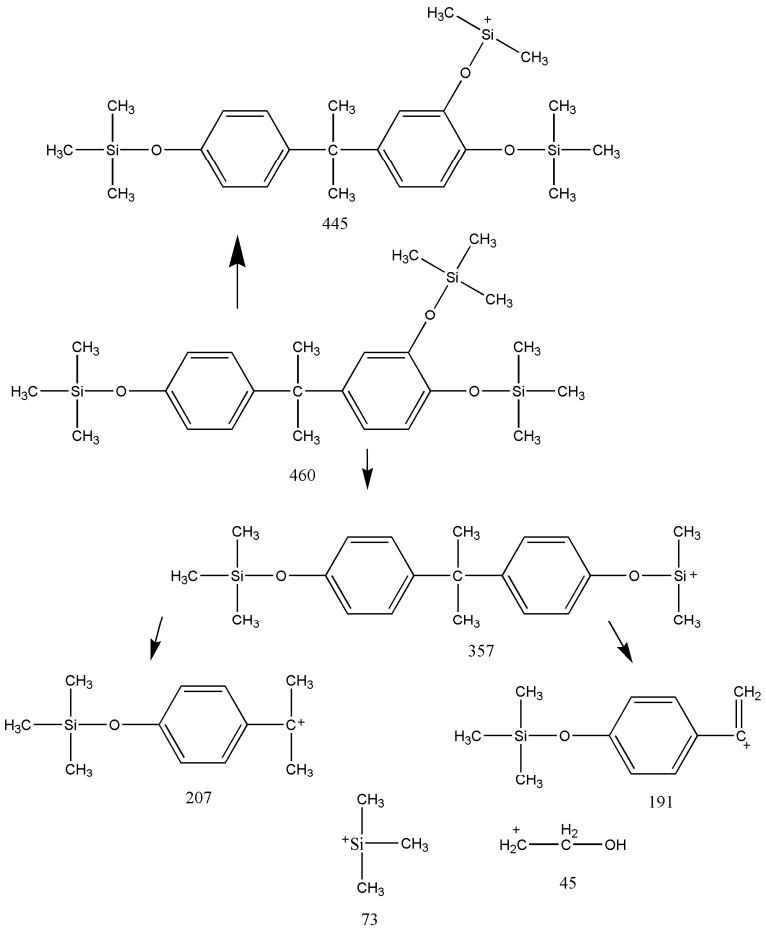
445
460
357
207
191
73
45

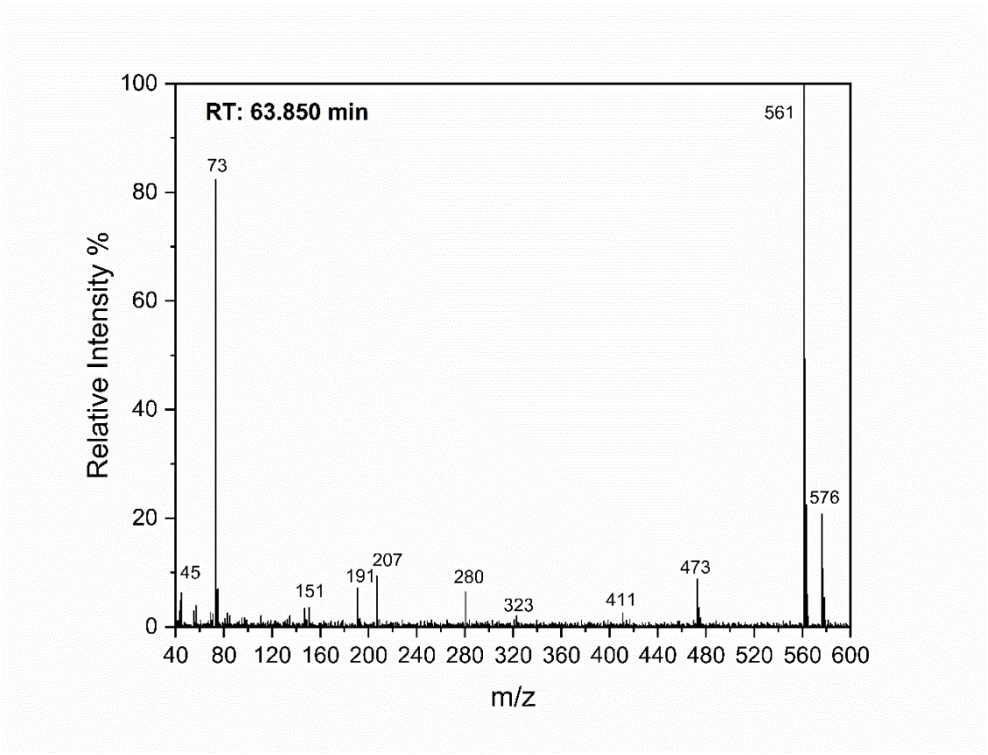
RT: 63.850 min
Relative Intensity %
m/z
73
561
576
45
151
191
207
280
323
411
473

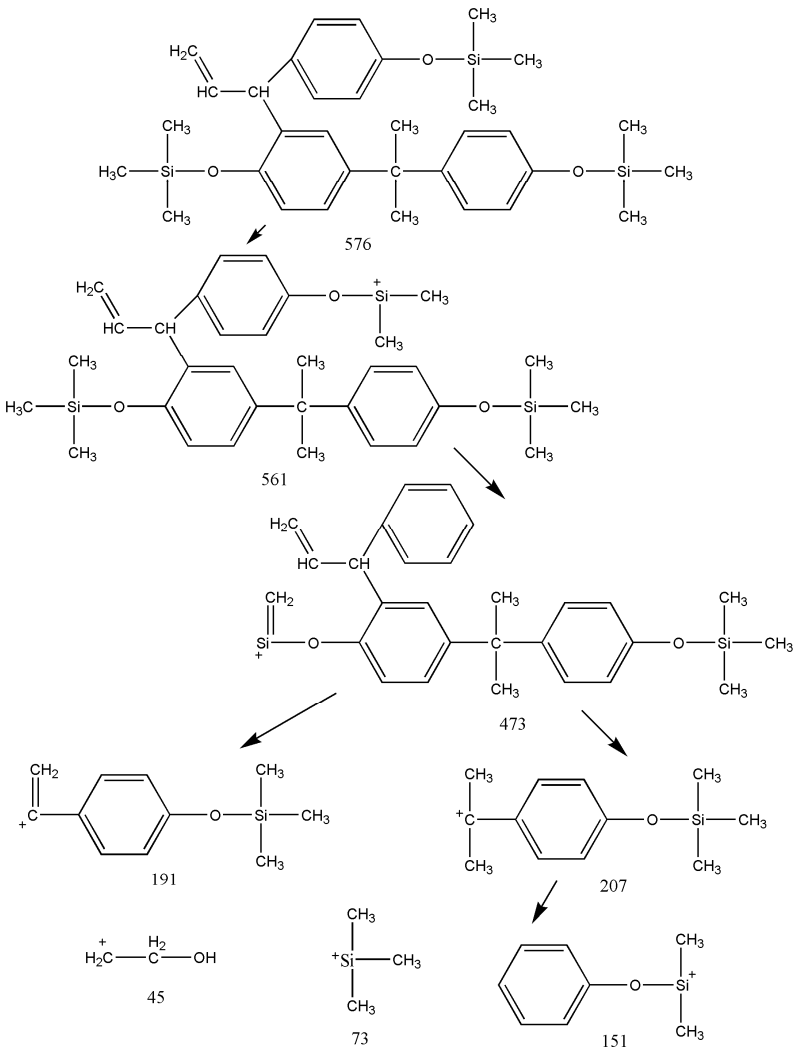
576
561
473
191
207
45
73
151

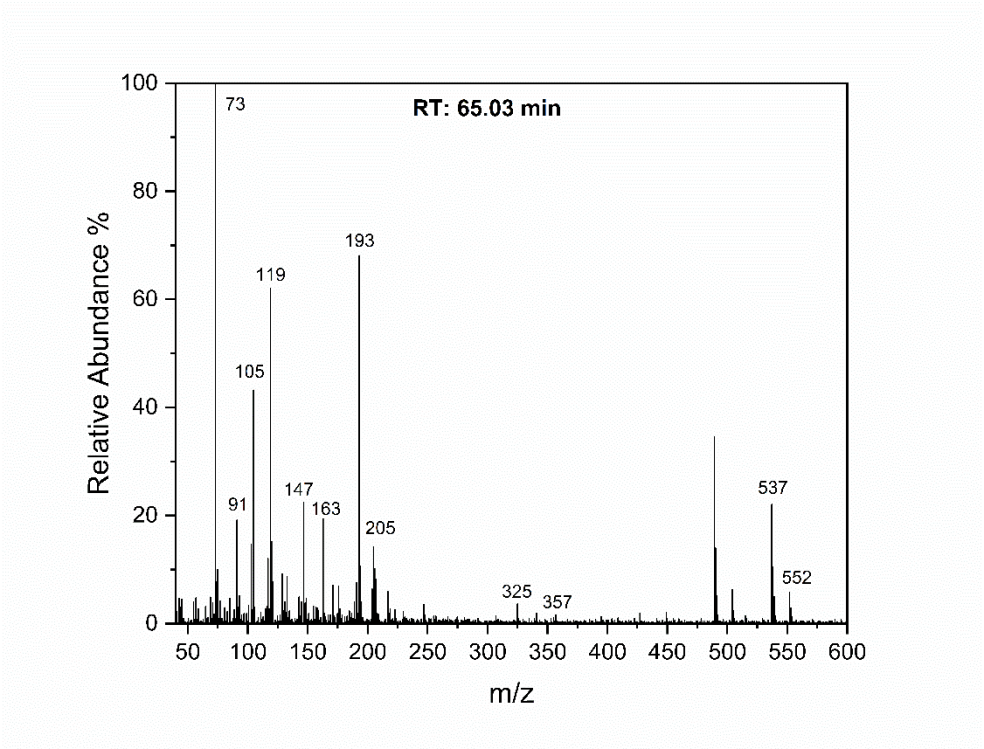
RT: 65.03 min
Relative Abundance %
m/z
73
193
119
105
147
91
163
205
325
357
537
552

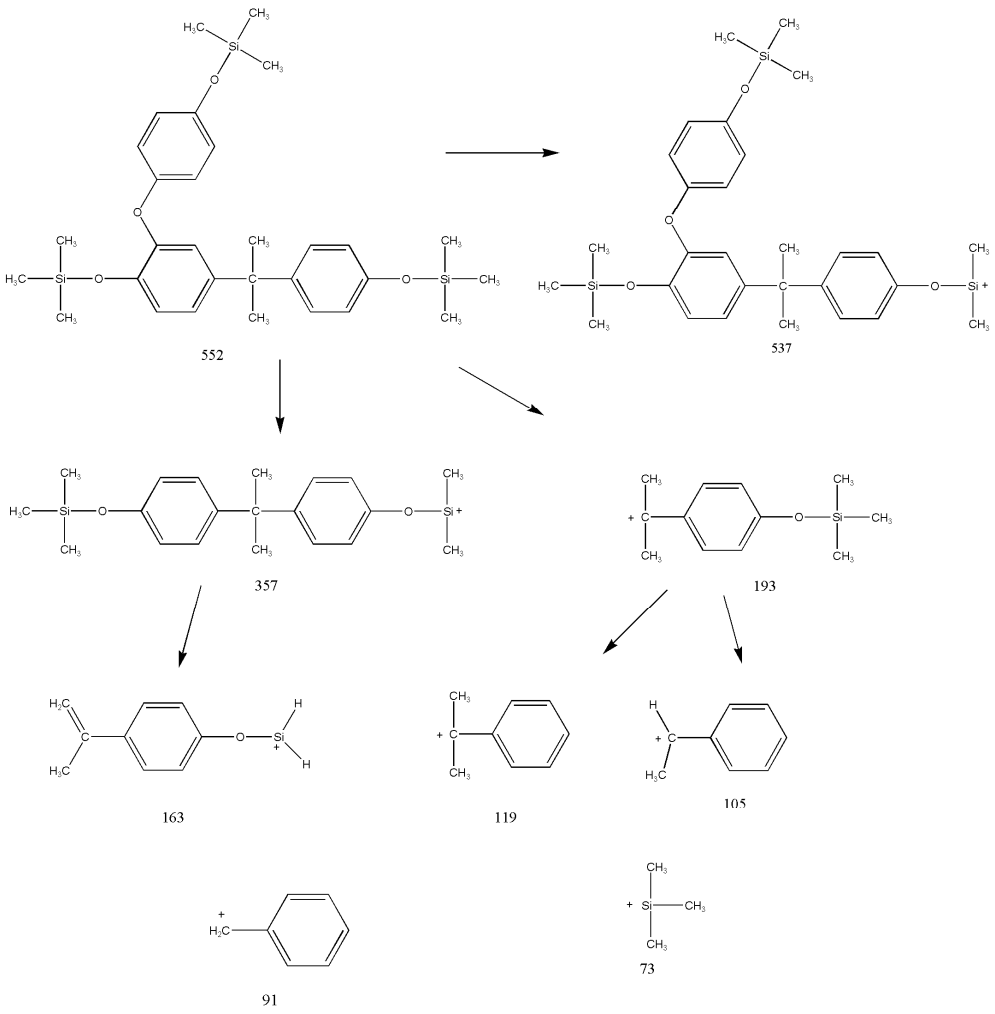
552
537
357
193
163
119
105
91
73

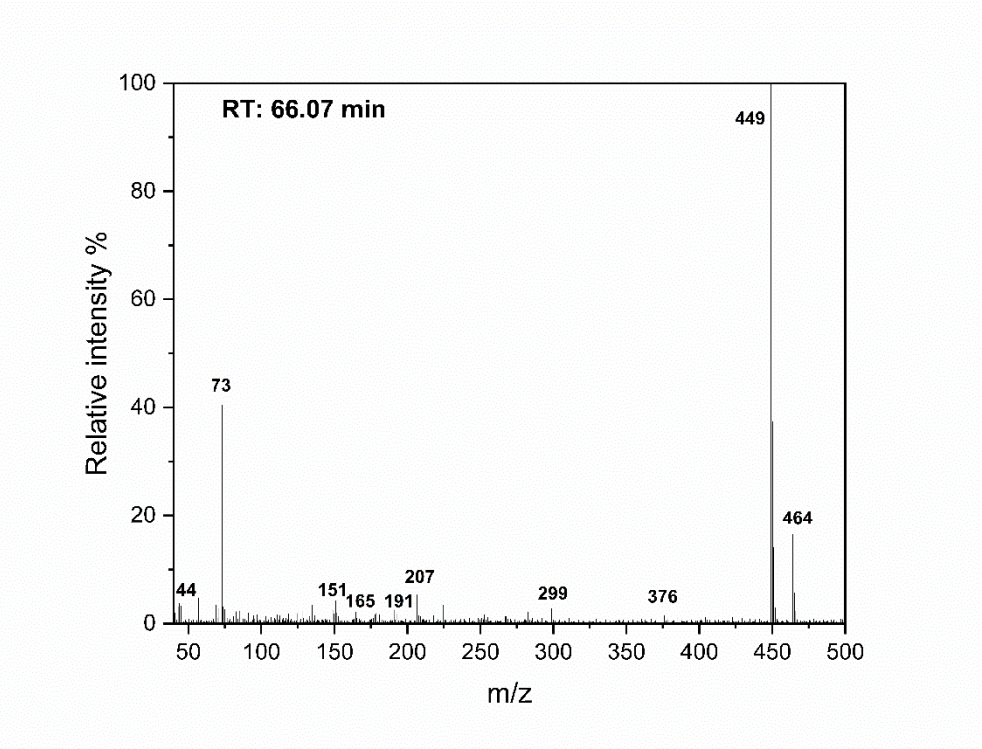

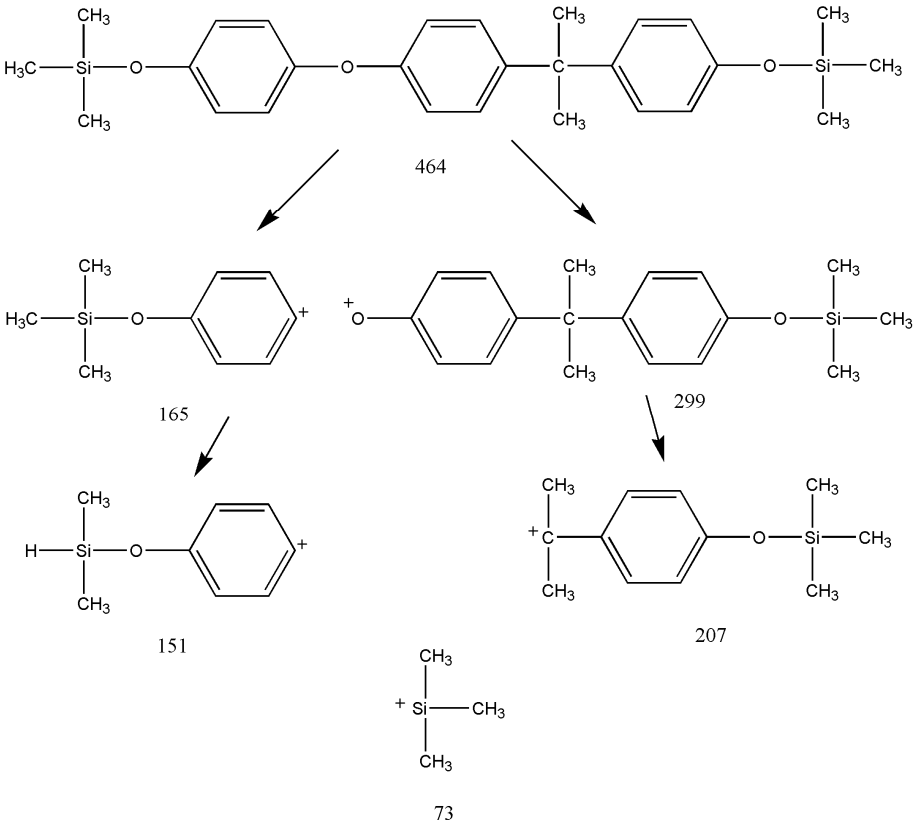

464

165

299

151

207

73

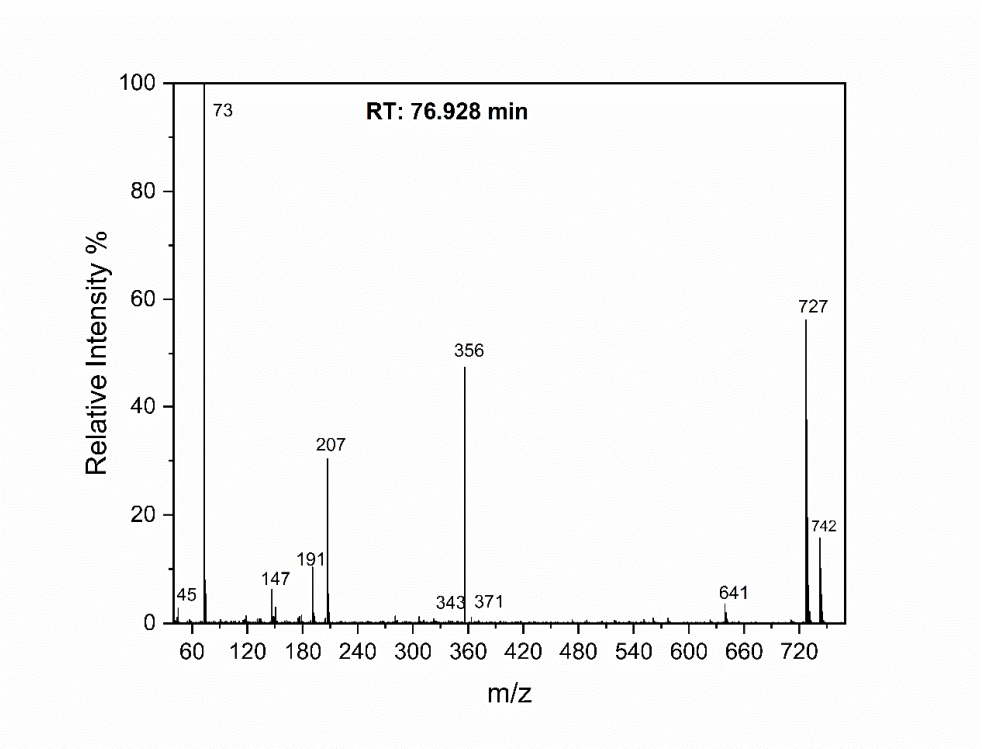
RT: 76.928 min
Relative Intensity %
m/z
73
45
147
191
207
343
356
371
641
727
742

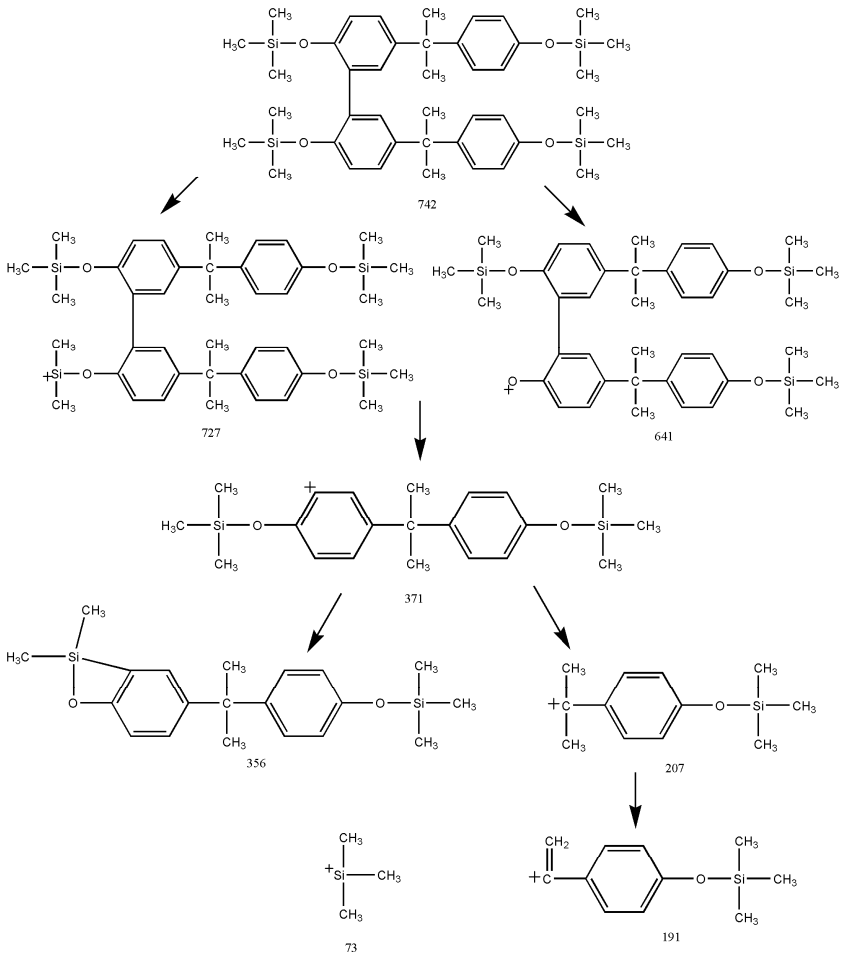
742
727
641
371
356
207
73
191

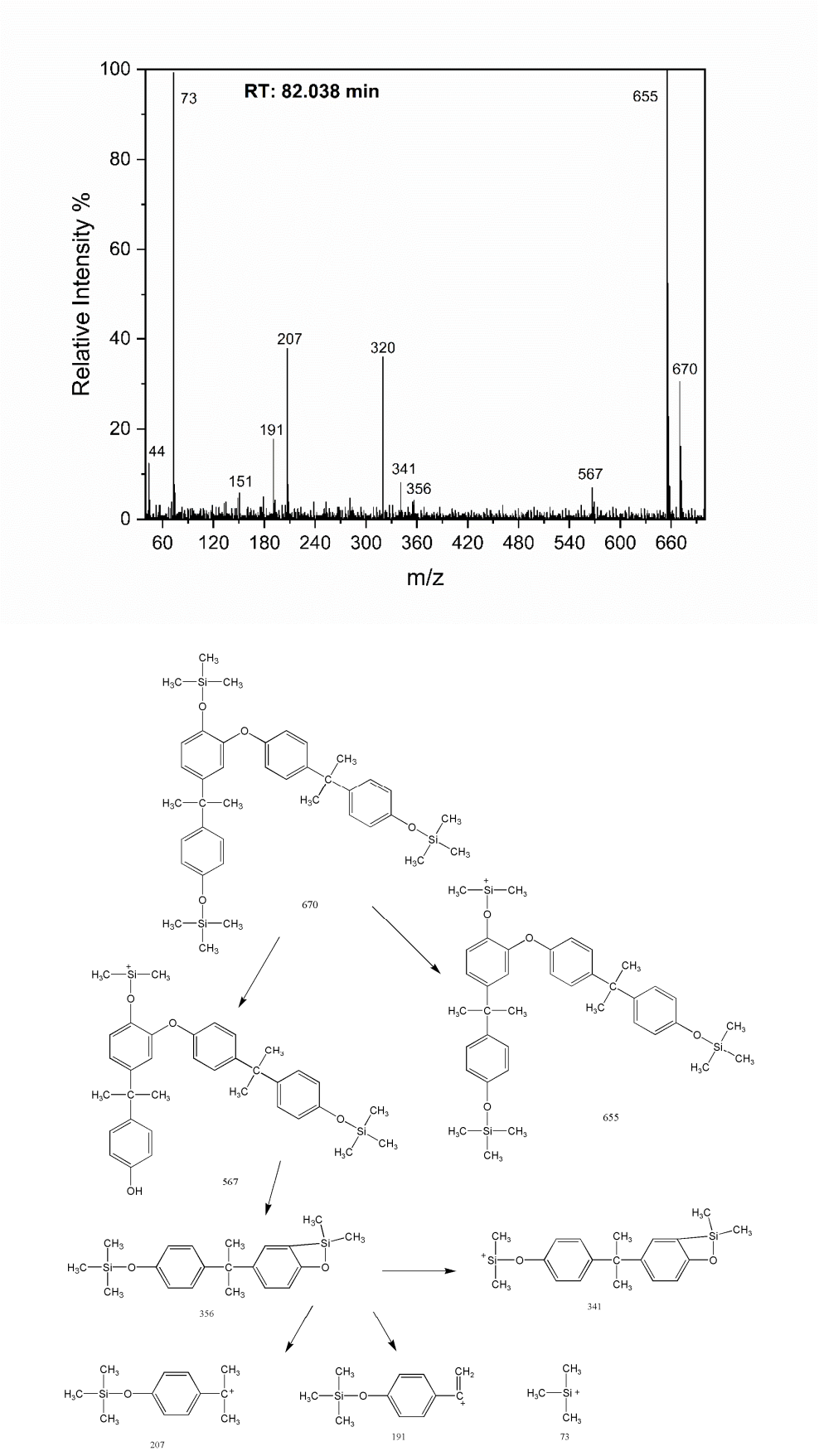

Figure S5. Proposed derivatized intermediates and their possible ion fragments

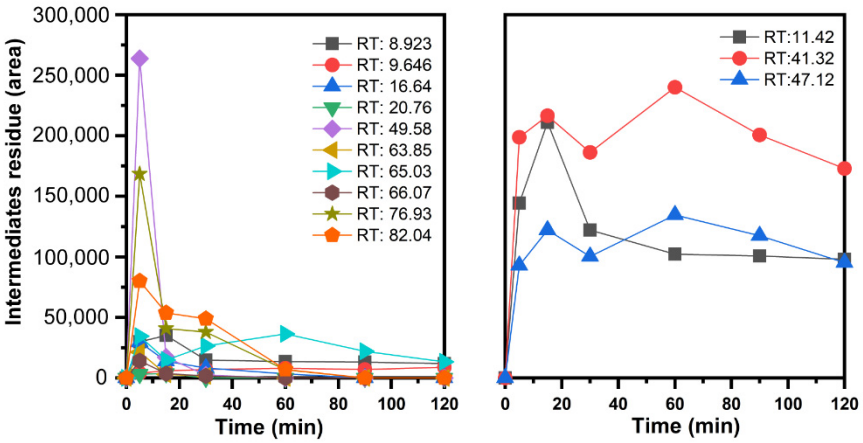

Figure S6. Intermediates residue in MnO_2/UV/PS process

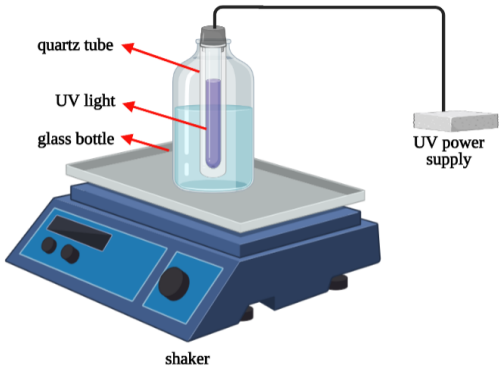

Figure S7. Schematic diagram of experimental device

Table S1. Parameters of BPA degradation following the pseudo-first-order kinetics with and without quenching (reaction time: 30 min; D: degradation efficiency)

Processes	**Scavengers**	**k (min^{-1})**	**R^2**	**D (%)**
	No quenching	0.0132	0.9724	34.0
	MeOH (1 M)	0.0061	0.9026	17.7
UV/MnO_2	TBA (1 M)	0.0051	0.9685	15.2
	FFA (5 mM)	0.0044	0.9732	13.1
	No quenching	0.0333	0.946	64.9
	MeOH (1 M)	0.0164	0.9631	39.6
MnO_2/PS	TBA (1 M)	0.0268	0.9934	55.0
	FFA (5 mM)	0.0313	0.9321	62.2
	No quenching	0.1178	0.9622	97.5
	MeOH (1 M)	0.0337	0.9723	65.7
UV/PS	TBA (1 M)	0.0297	0.963	61.2

	FFA (5 mM)	0.0109	0.9701	28.4
MnO_2/UV/PS	No quenching	0.2196	0.9471	99.3
	MeOH (1 M)	0.0469	0.9841	75.9
	TBA (1 M)	0.0631	0.9716	86.2
	FFA (5 mM)	0.0445	0.9547	74.1

Table S2. Degradation products of BPA under the MnO_2/UV/PS process identified using GC-MS

Retention time (min)	Molecular weight	Proposed structure	No.	References
8.92	108	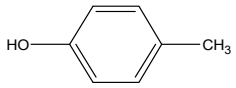	***P1***	—
9.65	138	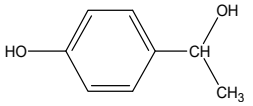	***P2***	—
11.42	124	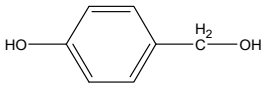	***P3***	—
16.63	134	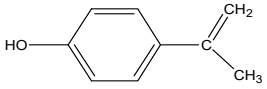	***P4***	[3-6]
20.76	136	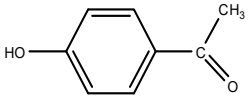	***P5***	[5, 7]
41.32	256	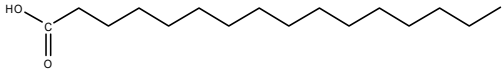	***P6***	—
46.23	228	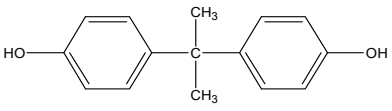	***BPA***	
47.12	280	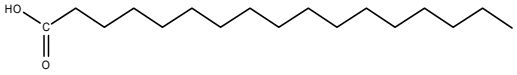	***P7***	—

49.58	244	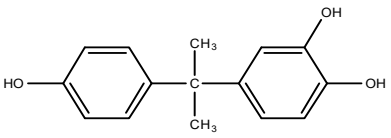	***P8***	[4, 5]
63.85	462	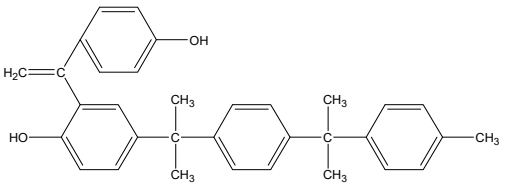	***P9***	—
65.03	336	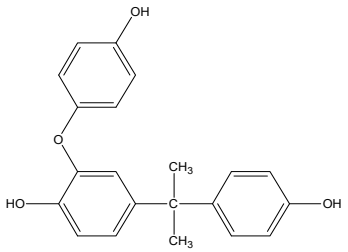	***P10***	—
66.07	320	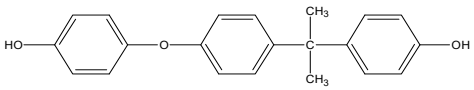	***P11***	[1]
76.93	454	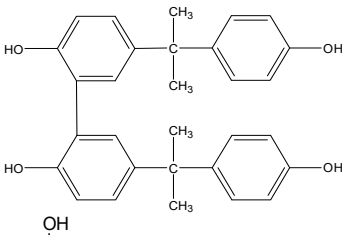	***P12***	[6, 8]
82.04	454	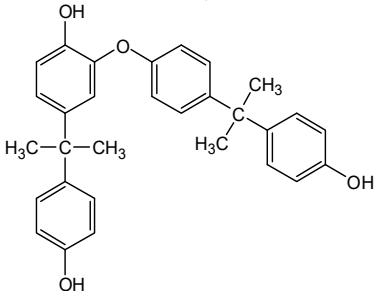	***P13***	[9, 10]

References

[1] J. Sharma, I. Mishra, D.D. Dionysiou, V. Kumar, Oxidative removal of Bisphenol A by UV-C/peroxymonosulfate (PMS): kinetics, influence of co-existing chemicals and degradation pathway, Chemical Engineering Journal 276 (2015) 193-204.
[2] K. Lin, W. Liu, J. Gan, Oxidative removal of bisphenol A by manganese dioxide: efficacy, products, and pathways, Environmental science & technology 43 (2009) 3860-3864.
[3] C. Guo, M. Ge, L. Liu, G. Gao, Y. Feng, Y. Wang, Directed synthesis of mesoporous TiO2 microspheres: catalysts and their photocatalysis for bisphenol A degradation, Environmental science & technology 44 (2010) 419-425.
[4] J. Lin, Y. Hu, L. Wang, D. Liang, X. Ruan, S. Shao, M88/PS/Vis system for degradation of bisphenol A: Environmental factors, degradation pathways, and toxicity evaluation, Chemical Engineering Journal 382 (2020) 122931.
[5] L. Liu, X. Xu, Y. Li, R. Su, Q. Li, W. Zhou, B. Gao, Q. Yue, One-step synthesis of “nuclear-shell” structure iron-carbon nanocomposite as a persulfate activator for bisphenol A degradation, Chemical Engineering Journal 382 (2020) 122780.
[6] E. de Freitas, G. Bubna, T. Brugnari, C. Kato, M. Nolli, T. Rauen, R. Moreira, R. Peralta, A. Bracht, C. de Souza, Removal of bisphenol A and evaluation of ecotoxicity of degradation products by laccases from Pleurotus ostreatus and Pleurotus pulmonarius, Chem. Eng. J 330 (2017) 1361-1369.
[7] M. Inoue, Y. Masuda, F. Okada, A. Sakurai, I. Takahashi, M. Sakakibara, Degradation of bisphenol A using sonochemical reactions, Water research 42 (2008) 1379-1386.
[8] C. Qi, X. Liu, Y. Li, C. Lin, J. Ma, X. Li, H. Zhang, Enhanced degradation of organic contaminants in water by peroxydisulfate coupled with bisulfite, Journal of hazardous materials 328 (2017) 98-107.
[9] L.M. Divya, G.K. Prasanth, K.G. Arun, C. Sadasivan, Bisphenol-A carbonate dimer is a more preferred substrate for laccase mediated degradation than the Biphenol-A in its monomeric and dimeric forms, International biodeterioration & biodegradation 135 (2018) 19-23.
[10] J. Yao, R. Qu, X. Wang, V.K. Sharma, A. Shad, A.A. Dar, Z. Wang, Visible light and fulvic acid assisted generation of Mn (III) to oxidize bisphenol A: The effect of tetrabromobisphenol A, Water research 169 (2020) 115273.